

VU Research Portal

The Pancharatnam-Berry phase for non-cyclic polarization changes

van Dijk, T.; Schouten, H.F.; Ubachs, W.M.G.; Visser, T.D.

published in

Optics Express
2010

DOI (link to publisher)

[10.1364/OE.18.010796](https://doi.org/10.1364/OE.18.010796)

document version

Publisher's PDF, also known as Version of record

[Link to publication in VU Research Portal](#)

citation for published version (APA)

van Dijk, T., Schouten, H. F., Ubachs, W. M. G., & Visser, T. D. (2010). The Pancharatnam-Berry phase for non-cyclic polarization changes. *Optics Express*, 18(10), 10796-10804. <https://doi.org/10.1364/OE.18.010796>

General rights

Copyright and moral rights for the publications made accessible in the public portal are retained by the authors and/or other copyright owners and it is a condition of accessing publications that users recognise and abide by the legal requirements associated with these rights.

- Users may download and print one copy of any publication from the public portal for the purpose of private study or research.
- You may not further distribute the material or use it for any profit-making activity or commercial gain
- You may freely distribute the URL identifying the publication in the public portal ?

Take down policy

If you believe that this document breaches copyright please contact us providing details, and we will remove access to the work immediately and investigate your claim.

E-mail address:

vuresearchportal.ub@vu.nl

The Pancharatnam-Berry phase for non-cyclic polarization changes

T. van Dijk^{1,*}, H.F. Schouten¹, W. Ubachs¹, and T.D. Visser^{1,2}

¹Dept. of Physics and Astronomy, and Laser Centre, VU University Amsterdam,
De Boelelaan 1081, 1081 HV Amsterdam, The Netherlands

²Also with Dept. of Electrical Engineering, Delft University of Technology,
Mekelweg 4, 2628 CD Delft, The Netherlands

[*t.d.visser@tudelft.nl](mailto:t.d.visser@tudelft.nl)

Abstract: We present a novel setup that allows the observation of the geometric phase that accompanies polarization changes in monochromatic light beams for which the initial and final states are different (so-called non-cyclic changes). This Pancharatnam-Berry phase can depend in a linear or in a nonlinear fashion on the orientation of the optical elements, and sometimes the dependence is singular. Experimental results that confirm these three types of behavior are presented. The observed singular behavior may be applied in the design of optical switches.

© 2010 Optical Society of America

OCIS codes: (230.5440) Polarization-selective devices; (260.5430) Polarization; (350.1370) Berry's phase; (350.5030) Phase

References and links

1. M.V. Berry, "Quantal phase factors accompanying adiabatic changes," *Proc. R. Soc. Lond. A* **392**, 45–57 (1984).
2. M.V. Berry, "Anticipations of the geometric phase," *Physics Today* **43**(12), 34–40 (1990).
3. J. Samuel and R. Bhandari, "General setting for Berry's phase," *Phys. Rev. Lett.* **60**, 2339–2342 (1988).
4. T.F. Jordan, "Berry phases for partial cycles," *Phys. Rev. A* **38**, 1590–1592 (1988).
5. A. Shapere and F. Wilczek (eds.), *Geometric Phases in Physics* (World Scientific, Singapore, 1989).
6. S. Pancharatnam, "Generalized theory of interference, and its applications," *Proc. Indian Acad. Sci. A* **44**, 247–262 (1956).
7. S. Pancharatnam, *Collected Works* (Oxford University Press, Oxford, 1975).
8. M.V. Berry, "The adiabatic phase and Pancharatnam's phase for polarized light," *J. Mod. Optics* **34**, 1401–1407 (1987).
9. M. Born and E. Wolf, *Principles of Optics: Electromagnetic Theory of Propagation, Interference and Diffraction of Light*, seventh (expanded) ed. (Cambridge University Press, Cambridge, 1999).
10. R. Bhandari, "Polarization of light and topological phases," *Phys. Rep.* **281**, 1–64 (1997).
11. P. Hariharan, "The geometric phase," in: *Progress in Optics* (E. Wolf, ed.) **48**, 149–201 (Elsevier, Amsterdam, 2005).
12. R. Bhandari and J. Samuel, "Observation of topological phase by use of a laser interferometer," *Phys. Rev. Lett.* **60**, 1211–1213 (1988).
13. T.H. Chyba, L.J. Wang, L. Mandel and R. Simon, "Measurement of the Pancharatnam phase for a light beam," *Opt. Lett.* **13**, 562–564 (1988).
14. H. Schmitzer, S. Klein and W. Dultz, "Nonlinearity of Pancharatnam's topological phase," *Phys. Rev. Lett.* **71**, 1530–1533 (1993).
15. R. Bhandari, "Observation of Dirac singularities with light polarization. I," *Phys. Lett. A* **171**, 262–266 (1992).
16. R. Bhandari, "Observation of Dirac singularities with light polarization. II," *Phys. Lett. A* **171**, 267–270 (1992).
17. R.C. Jones, "A new calculus for the treatment of optical systems," *J. Opt. Soc. Am.* **31**, 488–493 (1941).
18. T. van Dijk, H.F. Schouten and T.D. Visser, "Geometric interpretation of the Pancharatnam connection and non-cyclic polarization changes," submitted (2010).
19. C. Brosseau, *Fundamentals of Polarized Light* (Wiley, New York, 1998).

20. A.G. Wagh and V.C. Rakhecha, "On measuring the Pancharatnam phase. I. Interferometry," Phys. Lett. A **197**, 107–111 (1995).
21. J.F. Nye, *Natural Focusing and Fine Structure of Light* (IOP Publishing, Bristol, 1999).
22. G.I. Papadimitriou, C. Papazoglou and A.S. Pomportsis, *Optical Switching* (Wiley, Hoboken, 2007).

1. Introduction

In a seminal paper Berry [1] showed that when the Hamiltonian of a quantum mechanical system is adiabatically changed in a cyclic manner the system acquires, in addition to the usual dynamic phase, a so-called geometric phase. It was soon realized that such a phase is in fact quite general: it can also occur for non-adiabatic state changes and even in classical systems [2]– [5]. One of its manifestations is the Pancharatnam phase in classical optics [6]– [8]. The polarization properties of a monochromatic light beam can be represented by a point on the Poincaré sphere [9]. When, with the help of optical elements such as polarizers and retarders, the state of polarization is made to trace out a closed contour on the sphere, the beam acquires a geometric phase. This *Pancharatnam-Berry phase*, as it is nowadays called, is equal to half the solid angle of the contour subtended at the origin of the sphere [10]– [12]. The various kinds of behavior of the geometric phase for cyclic polarization changes have been studied extensively [13]– [16].

In this paper we study the geometric phase for *non-cyclic* polarization changes, i.e. polarization changes for which the initial state and the final state are different. Such changes correspond to non-closed paths on the Poincaré sphere. The geometric phase can depend in a linear, a non-linear or in a singular fashion on the orientation of the optical elements. Experimental results that confirm these three types of behavior are presented. The observed singular behavior may be applied in the design of fast optical switches.

The states of polarization, A and B , of two monochromatic light beams can be represented by the Jones vectors [17]

$$\mathbf{E}_A = \begin{pmatrix} \cos \alpha_A \\ \sin \alpha_A e^{i\theta_A} \end{pmatrix}, \quad (0 \leq \alpha_A \leq \pi/2; -\pi \leq \theta_A \leq \pi), \quad (1)$$

$$\mathbf{E}_B = e^{i\gamma} \begin{pmatrix} \cos \alpha_B \\ \sin \alpha_B e^{i\theta_B} \end{pmatrix}, \quad (0 \leq \alpha_B \leq \pi/2; -\pi \leq \theta_B \leq \pi). \quad (2)$$

Since only relative phase differences are of concern, the overall phase of \mathbf{E}_A in Eq. (1) is taken to be zero. According to Pancharatnam's connection [8, 18] the two states are in phase when their superposition yields a maximal intensity, i.e., when

$$|\mathbf{E}_A + \mathbf{E}_B|^2 = |\mathbf{E}_A|^2 + |\mathbf{E}_B|^2 + 2 \operatorname{Re}(\mathbf{E}_A \cdot \mathbf{E}_B^*) \quad (3)$$

reaches its greatest value, and hence

$$\operatorname{Im}(\mathbf{E}_A \cdot \mathbf{E}_B^*) = 0, \quad (4)$$

$$\operatorname{Re}(\mathbf{E}_A \cdot \mathbf{E}_B^*) > 0. \quad (5)$$

These two conditions uniquely determine the phase γ , except when A and B are orthogonal.

2. Non-cyclic polarization changes

We study a series of polarization changes for which the successive states are assumed to be in phase. To illustrate the rich behavior of the geometric phase, consider a beam in an arbitrary initial state A , that passes through a linear polarizer whose transmission axis is under an angle ϕ_1 with the positive x -axis. This results in a second state B that lies on the equator of the

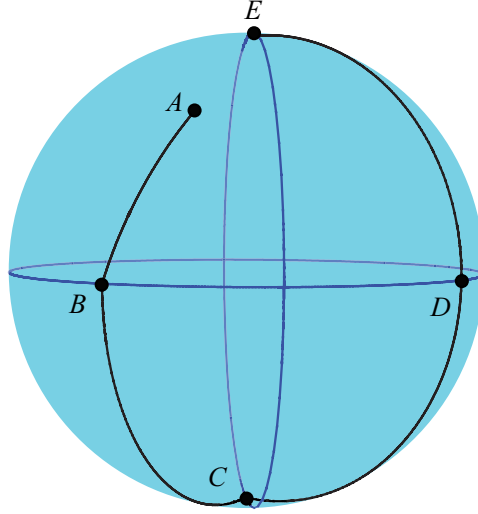


Fig. 1. Non-closed path $ABCDE$ on the Poincaré sphere for a monochromatic light beam that passes through a sequence of polarizers and compensators.

Poincaré sphere (see Fig. 1). Next the beam passes through a suitably oriented compensator, which produces a third, left-handed circularly polarized state C on the south pole. The action of a second linear polarizer, with orientation angle ϕ_2 , creates state D on the equator. Finally, a second compensator causes the polarization to become right-handed circular, corresponding to the state E on the north pole. These successive manipulations can be described with the help of Jones calculus [17, 19]. The matrix for a linear polarizer whose transmission axis is under an angle ϕ with the positive x -axis equals

$$\mathbf{P}(\phi) = \begin{pmatrix} \cos^2 \phi & \cos \phi \sin \phi \\ \cos \phi \sin \phi & \sin^2 \phi \end{pmatrix}, \quad (6)$$

whereas the matrix for a compensator (“retarder”) with a fast axis under an angle θ with the positive x -axis, which introduces a phase change δ between the two field components is

$$\mathbf{C}(\delta, \theta) = \begin{pmatrix} \cos(\delta/2) + i \sin(\delta/2) \cos(2\theta) & i \sin(\delta/2) \sin(2\theta) \\ i \sin(\delta/2) \sin(2\theta) & \cos(\delta/2) - i \sin(\delta/2) \cos(2\theta) \end{pmatrix}. \quad (7)$$

The (unnormalized) Jones vector for the final state E thus equals

$$\mathbf{E}_E = \mathbf{C}(\pi/2, \phi_2 - \pi/4) \cdot \mathbf{P}(\phi_2) \cdot \mathbf{C}(-\pi/2, \phi_1 - \pi/4) \cdot \mathbf{P}(\phi_1) \cdot \mathbf{E}_A. \quad (8)$$

Hence we find for the normalized states the expressions

$$\mathbf{E}_B = \mathbf{P}(\phi_1) \cdot \mathbf{E}_A = T(A, \phi_1) \begin{pmatrix} \cos \phi_1 \\ \sin \phi_1 \end{pmatrix}, \quad (9)$$

$$\mathbf{E}_C = \mathbf{C}(-\pi/2, \phi_1 - \pi/4) \cdot \mathbf{E}_B = T(A, \phi_1) e^{-i\phi_1} \begin{pmatrix} 1/\sqrt{2} \\ i/\sqrt{2} \end{pmatrix}, \quad (10)$$

$$\mathbf{E}_D = \mathbf{P}(\phi_2) \cdot \mathbf{E}_C = T(A, \phi_1) e^{i(\phi_2 - \phi_1)} \begin{pmatrix} \cos \phi_2 \\ \sin \phi_2 \end{pmatrix}, \quad (11)$$

$$\mathbf{E}_E = \mathbf{C}(\pi/2, \phi_2 - \pi/4) \cdot \mathbf{E}_D = T(A, \phi_1) e^{i(2\phi_2 - \phi_1)} \begin{pmatrix} 1/\sqrt{2} \\ -i/\sqrt{2} \end{pmatrix}, \quad (12)$$

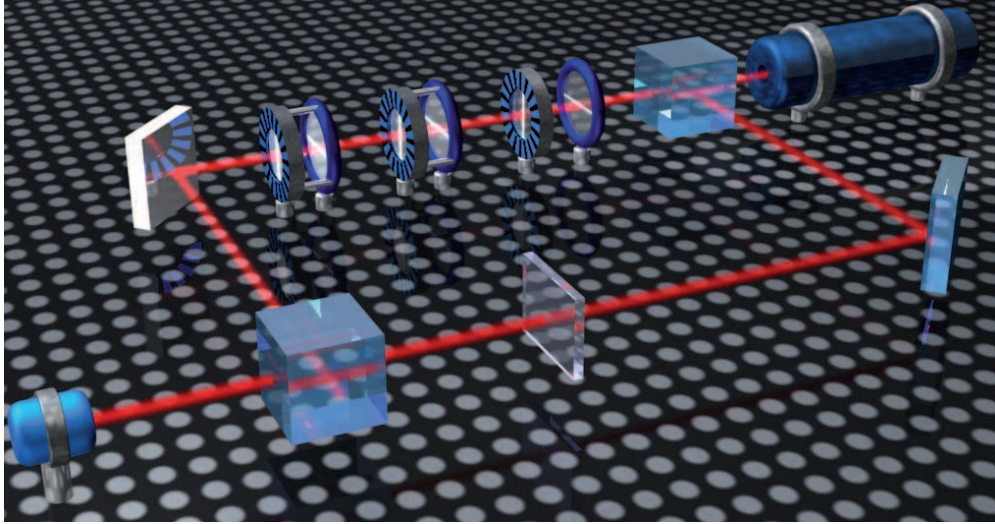


Fig. 2. Sketch of the Mach-Zehnder setup. The light from a He-Ne laser (right-hand top) is split into two beams. All polarizing elements are placed in the upper arm, the lower arm only contains a gray filter. The compensators are depicted with striped holders, the linear polarizers with non-striped holders. The last two pairs of elements are mounted together. The interference pattern of the recombined beams is recorded with either a photo diode or a CCD camera (left-hand bottom).

where

$$T(A, \phi_1) = \frac{\cos \alpha_A \cos \phi_1 + \sin \alpha_A e^{i\theta_A} \sin \phi_1}{|\cos \alpha_A \cos \phi_1 + \sin \alpha_A e^{i\theta_A} \sin \phi_1|} \quad (13)$$

is the (normalized) projection of the initial state A onto the state $(\cos \phi_1, \sin \phi_1)^T$. Although in general the output produced by a compensator is not in phase with the input, it is easily verified with the help of Eqs. (4) and (5) that in this example all consecutive states are indeed in phase. Hence it follows from Eq. (12), that we can identify the quantity

$$\Psi = \arg[T(A, \phi_1) e^{i(2\phi_2 - \phi_1)}] \quad (14)$$

as the geometric phase of the final state E . When a beam in this state is combined with a beam in state A , the intensity equals [cf. Eq. (3)]

$$|\mathbf{E}_A|^2 + |\mathbf{E}_E|^2 + 2\text{Re}(\mathbf{E}_A \cdot \mathbf{E}_E^*) = 1 + |T(A, \phi_1)|^2 + 2H(A, \phi_1) \cos(2\phi_2 - \phi_1 + \phi_H), \quad (15)$$

where

$$H(A, \phi_1) e^{i\phi_H} = T^*(A, \phi_1) \mathbf{E}_A \cdot \begin{pmatrix} 1/\sqrt{2} \\ i/\sqrt{2} \end{pmatrix}, \quad (16)$$

and with $H(A, \phi_1) \in \mathbb{R}^+$. In the next section we investigate the dependence of the geometric phase of the final state E on the initial state A , and as a function of the two orientation angles ϕ_1 and ϕ_2 , and experimentally test our predictions.

3. Experimental method

The above sequence of polarization changes can be realized with a Mach-Zehnder interferometer (see Fig. 2). The output of a He-Ne laser operating at 632.8 nm is divided into two beams. The beam in one arm passes through a linear polarizer and a quarter-wave plate. This produces state *A*. By rotating the plate, this initial polarization state can be varied. Next the field passes through a polarizer $P(\phi_1)$ that creates state *B*, and a compensator C_1 , resulting in state *C*. A polarizer $P(\phi_2)$ produces state *D*, and a compensator C_2 creates the final state *E*. The elements $P(\phi_1), C_1$ and $P(\phi_2), C_2$ are joined pairwise to ensure that their relative orientation remains fixed when the angles ϕ_1 and ϕ_2 are varied, and the resulting states are circularly polarized. The field in the other arm is attenuated by a gray filter in order to increase the sharpness of the fringes. The fields in both arms are combined, and the ensuing interference pattern is detected with the help of a detector. Both a photodiode and a CCD camera are used.

On varying the angle ϕ_2 , the intensity in the upper arm of Fig. 2 remains unchanged and the changes in the diffraction pattern can be recorded with a photodiode. However, when the angle ϕ_1 is varied, the intensity in that arm changes. The shape of the interference pattern then changes as well, and the geometric phase can only be observed by measuring a shift of the *entire* pattern with a CCD camera [20].

One has to make sure that rotating the optical elements does not affect the optical path length and introduces an additional dynamic phase. This was achieved by an alignment procedure in which the invariance of the interference pattern for 180° rotations of the linear polarizers was exploited. Mechanical vibrations were minimized by remotely controlling the optical elements.

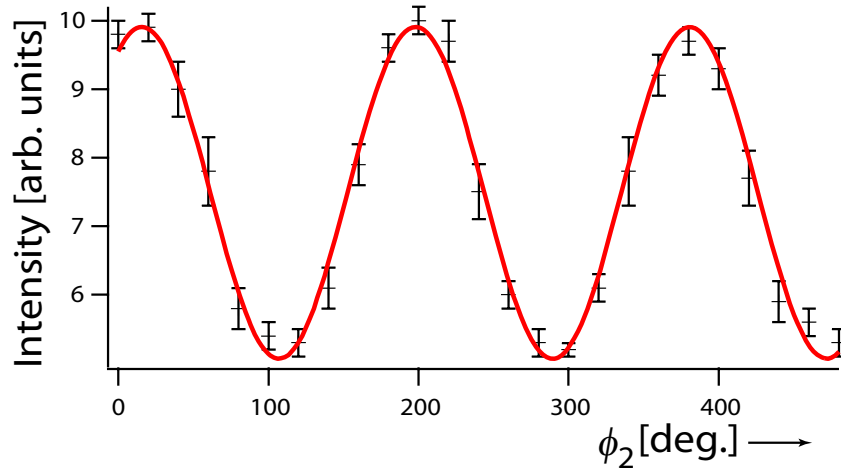


Fig. 3. Measured intensity as a function of the orientation angle ϕ_2 . The solid curve is a fit of the measured data to the function $C_1 + C_2 \cos(2\phi_2 + C_3)$. The vertical symbols indicate error bars.

4. Experimental results

The dependence of the geometric phase of the final state *E* on the orientation angles ϕ_1 and ϕ_2 of the two polarizers is markedly different. It is seen from Eq. (14) that the phase is proportional to ϕ_2 . This linear behavior is illustrated in Fig. 3 in which the intensity observed with a photodiode is plotted as a function of the angle ϕ_2 . The solid curve is a fit of the data to the function $C_1 + C_2 \cos(2\phi_2 + C_3)$, with C_1 , C_2 and C_3 all constants [cf. Eq. (15)]. The excellent

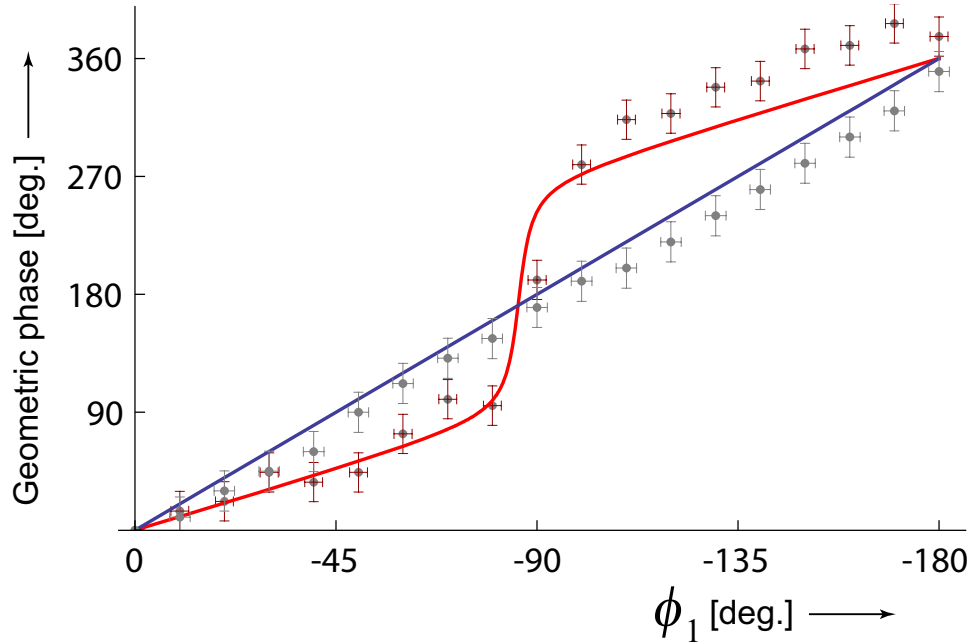


Fig. 4. Geometric phase of the final state E when the initial state A coincides with the north pole (blue curve), and when A lies between the equator and the north pole (red curve), both as a function of the orientation angle ϕ_1 . The solid curves are theoretical predictions [Eq. (14)], the dots and error bars represent measurements. In this example $\phi_2 = 0$.

agreement between the measurements and the fitted curve show that the geometric phase Ψ indeed increases twice as fast as the angle ϕ_2 .

In order to investigate the change $\Delta\Psi$ when the angle ϕ_1 is varied from 0° to 180° (after which the polarizer returns to its original state), let us first assume that the initial state A coincides with the north pole (i.e., $\alpha_A = \pi/4$, $\theta_A = -\pi/2$). In that case the path on the Poincaré sphere is closed and we find from Eq. (14) that $\Psi = 2(\phi_2 - \phi_1)$. The solid angle of the traversed path is now $4(\phi_2 - \phi_1)$. Thus we see that in that case we retrieve Pancharatnam's result that the acquired geometric phase for a closed circuit equals half the solid angle of the circuit subtended at the sphere's origin. Hence, on rotating ϕ_1 over 180° , the accrued geometric phase $\Delta\Psi$ equals 360° . This predicted behavior is indeed observed, see Fig. 4 (blue curve). For an arbitrary initial state on the northern hemisphere [in this example, with Stokes vector $(0.99, -0.14, 0.07)$] the behavior is nonlinear, but again we find that $\Delta\Psi = 360^\circ$ after the first polarizer has been rotated over 180° , see Fig. 4 (red curve).

Let us next assume that the initial state A coincides with the south pole ($\alpha_A = \pi/4$, $\theta_A = \pi/2$). In that case, Eq. (14) yields $\Psi = 2\phi_2$. Since this is independent of ϕ_1 , a rotation of ϕ_1 over 180° results in $\Delta\Psi = 0^\circ$. This corresponds to the blue curve in Fig. 5. For an arbitrary initial state on the southern hemisphere [in this example, with Stokes vector $(0.93, 0.23, -0.28)$] the geometric phase does vary with ϕ_1 , but again $\Delta\Psi = 0^\circ$ after a 180° rotation of the polarizer $P(\phi_1)$, see Fig. 5 (red curve). So, depending on the initial polarization state A , topologically different types of behavior can occur, with either $\Delta\Psi = 0^\circ$ or $\Delta\Psi = 360^\circ$ after half a rotation of the polarizer $P(\phi_1)$. This implies that on moving the state A across the Poincaré sphere a continuous change from one type of behavior to another is not possible. A discontinuous change in behavior can

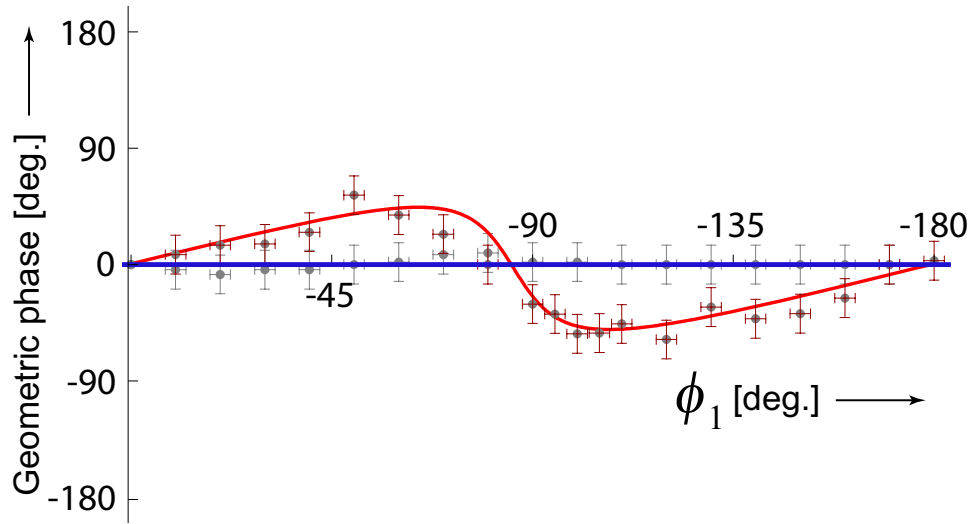


Fig. 5. Geometric phase of the final state E when the initial state A coincides with the south pole (blue curve), and when A lies between the equator and the south pole (red curve), both as a function of the orientation angle ϕ_1 . The solid curves are theoretical predictions [Eq. (14)], the dots and error bars represent measurements. In this example $\phi_2 = 0$.

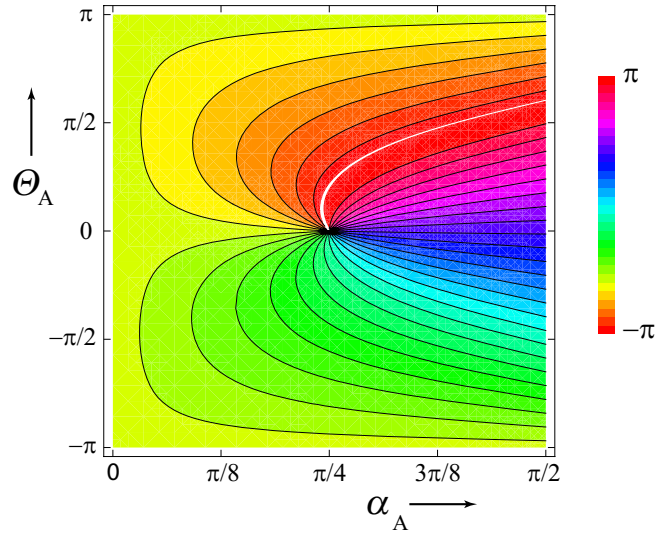


Fig. 6. Color-coded plot of the phase of the final state E as a function of the initial state A as described by the two parameters α_A and θ_A [cf. Eq. (1)]. In this example $\phi_1 = 3\pi/4$, and $\phi_2 = 1.8$.

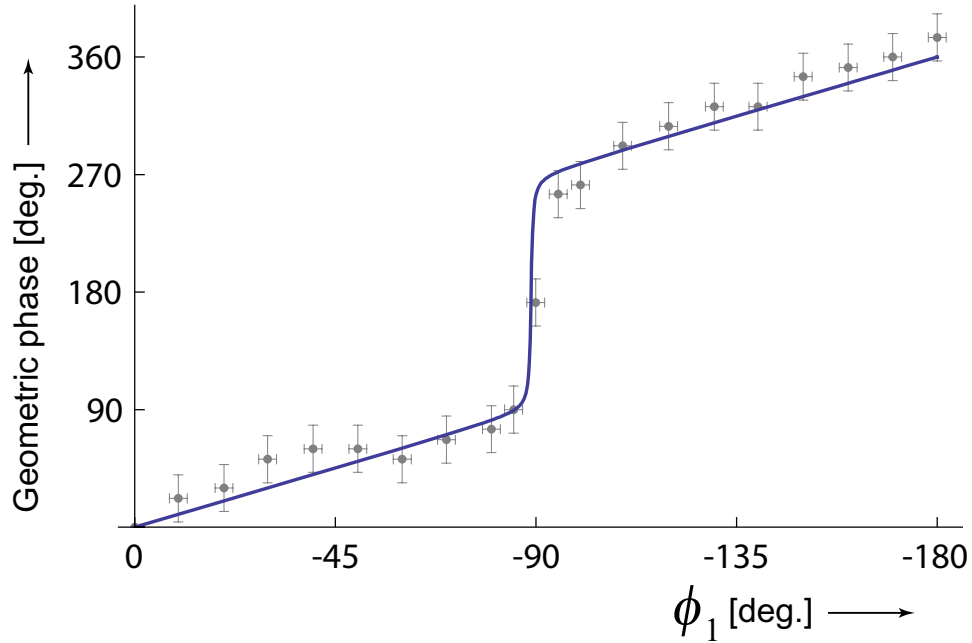


Fig. 7. Singular behavior of the geometric phase of the final state E when the initial state A lies on the equator, as a function of the orientation angle ϕ_1 . The solid curve is a theoretical prediction [Eq. (14)], the dots and error bars represent measurements. In this example $\theta_A = 0.27$, $\alpha_A = 0.0$ and $\phi_2 = 0$.

only occur when the geometric phase Ψ is singular. This happens when the first state A and the second state B are directly opposite to each other on the Poincaré sphere (and form a pair of “anti-podal points”). They are then orthogonal and the phase of the final state E is singular [21]. Indeed, when the state A lies on the equator ($\theta_A = 0$) then $\Psi = 2\phi_2 - \phi_1$, or $\Psi = 2\phi_2 - \phi_1 + \pi$, except when A and B are opposite. In that case Ψ is singular and undergoes a π phase jump. In Fig. 6 this occurs for the point ($\alpha_A = \pi/4$, $\theta_A = 0$) at which all the different phase contours intersect. In other words, when A moves across the equator, the geometric phase as a function of the angle ϕ_1 is singular and a transition from one type of behavior (with $\Delta\Psi = 360^\circ$) to another type (with $\Delta\Psi = 0^\circ$) occurs. This singular behavior, resulting in a 180° discontinuity of the geometric phase was indeed observed, see Fig. 7. Notice that although the depicted jump equals 180° , in our experiment it cannot be discerned from a -180° discontinuity. Whereas a positive jump results in $\Delta\Psi = 360^\circ$ after a 180° rotation of the first polarizer, a negative jump yields $\Delta\Psi = 0^\circ$. In that sense the singular behavior forms an intermediate step between the two dependencies shown in Figs. 4 and 5.

The ability to produce a 180° phase jump by means of a much smaller variation in ϕ_1 can be employed to cause a change from constructive interference to destructive interference when the beam is combined with a reference beam. Clearly, such a scheme can be used for fast optical switching [22].

5. Conclusions

In summary, we have presented a new Mach-Zehnder type setup with which the geometric phase that accompanies non-cyclic polarization changes can be observed. The geometric phase

can exhibit linear, nonlinear or singular behavior. Excellent agreement between the predicted and observed behavior was obtained.

Acknowledgements

The authors wish to thank Jacques Bouma for technical assistance, and The Netherlands Foundation for Fundamental Research of Matter (FOM) for financial support. TvD is supported by the Netherlands Organisation for Scientific Research (NWO) through a “Toptalent scholarship.”